EPR Studies of SiBNC Preceramic Polymers and Ceramic Employing Isotope Labeling

Yee Hwa Sehlleier,[†] Yasar Akdogan,[‡] Aswin Verhoeven,[†] Emil Roduner,[‡] and Martin Jansen*,[†]

Max Planck Institute for Solid State Research, Heisenbergstr. 1, D-70569 Stuttgart, Germany, and Institute of Physical Chemistry, University of Stuttgart, Pfaffenwaldring 55, D-70569 Stuttgart, Germany

Received July 10, 2008. Revised Manuscript Received October 2, 2008

The magnetic properties of amorphous preceramic polymer and ceramic samples with a composition of silicon, boron, nitrogen, and carbon were investigated. The incorporation of carbon atoms into the ternary SiBN system leads to an increase of the concentration of unpaired electrons. In the present article, this paramagnetism is intensively studied. EPR and SQUID measurements show that the concentration of paramagnetic centers is increased when the sample is pyrolyzed at higher temperatures. Previously performed solid-state NMR experiments demonstrate that the carbon structure undergoes a transformation during pyrolysis. This process may be directly related to the amount of unpaired electrons in the sample. In order to identify the location of the unpaired electrons, EPR experiments on isotope labeled SiBNC ceramics were compared with experiments on unlabeled material. Different pyrolysis temperatures and isotope labeling lead to a variation of the intensity and the shape of the EPR line. The isotope enrichment causes a broadening of the EPR resonance line, which is consistent with the idea that the small polycyclic aromatic carbons with corresponding nitrogen bridges act as sinks for the unpaired electron. As a consequence, unresolved hyperfine couplings to ^{13}C and ^{15}N nuclei lead to a broader line.

1. Introduction

Recently, a significant amount of effort has been invested in attempts to achieve new classes of high performance ceramic materials. Amorphous ceramic materials based on silicon, boron, carbon, and nitrogen elements are of particular interest because of their superb physical and chemical properties.[1−3] The polymerization of an organic single source precursor molecule and subsequent pyrolysis is the only known procedure for obtaining an almost homogeneous ceramic material of this type. These are promising for industrial applications because of their low density, high thermal stability, cheap starting materials, mechanical strength, and chemical resistance against oxidation at elevated temperatures.[4] The presence of carbon in the network improves the mechanical properties of precursor-derived SiBNC ceramics as compared to the ternary ceramic SiBN. The characterization of these pyrolyzed ceramics was performed by several methods in earlier studies.[5−7] To understand the effect of the incorporation of carbon atoms into the SiBN network, it is essential to obtain information on how the material, particularly the carbon environment, transforms from the polymer stage to the final ceramic stage. One effect of the presence of carbon in the network is the appearance of unpaired electrons during pyrolysis. EPR is obviously the most powerful tool to study the occurrence of paramagnetic centers. Thus, in the past, several samples were already studied with EPR to determine the properties of paramagnetic centers in carbon-containing ceramics.[8,9] However, neither the origin nor the location of the paramagnetic centers is yet fully understood. Therefore, it was decided to carry out EPR studies employing isotope labeled SiBNC ceramics with the aim of understanding where paramagnetic centers are located in these samples. By preparing various samples, in both isotope labeled and unlabeled forms, it becomes possible to study unresolved hyperfine couplings to the introduced isotopes. The study of the preceramic polymer stages at intermediate pyrolysis temperatures (673 and 873 K) and the final ceramic (1673 K) may yield clues on the origin of the unpaired electrons. Furthermore, the investigation of the EPR line shape, line width, *g*-value, and spin concentration can give valuable information to understand the magnetic properties of the sample. The EPR experiments are combined with SQUID measurements to study the temperature dependent magnetic susceptibility which may offer supplementary insights into interactions between electron spins. These results are compared with solid-state NMR measurements to examine the structural

* To whom correspondence should be addressed. E-mail: m.jansen@fkf.mpg.de.
[†] Max Planck Institute for Solid State Research.
[‡] University of Stuttgart.

(1) Baldus, H. P.; Jansen, M. *Science* **1999**, *285*, 699.
(2) Baldus, H. P.; Jansen, M. *Angew. Chem., Int. Ed. Engl.* **1997**, *36*, 328.
(3) Haberecht, J.; Krumeich, F.; Grützmacher, H.; Nesper, R. *Chem. Mater.* **2004**, *16*, 418.
(4) Jansen, M.; Jäschke, B.; Jäschke, T. *Struct. Bonding (Berlin)* **2002**, *101*, 137.
(5) Ngheim, Q. D.; Jeon, J. K.; Hong, L. Y.; Kim, D. P. *J. Organomet. Chem.* **2003**, *688*, 27.
(6) Haberecht, J.; Nesper, R.; Grützmacher, H. *Chem. Mater.* **2005**, *17*, 2340.
(7) Sehlleier, Y. H.; Verhoeven, A.; Jansen, M. *J. Mater. Chem.* **2007**, *17*, 4316.
(8) Jeschke, G.; Kroschel, M.; Jansen, M. *J. Non-Cryst. Solids* **1999**, *260*, 216.
(9) Berger, F.; Müller, A.; Aldinger, F.; Müller, K. *Z. Anorg. Allg. Chem.* **2005**, *631*, 355.

10.1021/cm801889w CCC: $40.75
Published on Web 11/17/2008

Table 1. Information about the Samples with Labeling Schemes and Pyrolysis Temperatures

sample	labeling	pyrolysis temperature
1a	unlabeled	673 K
2a	unlabeled	873 K
2b	^{13}C, ^{15}N-labeled	873 K
3a	unlabeled	1673 K
3b	^{13}C, ^{15}N-labeled	1673 K

transformation of the material and to study the relation between the carbon structure and the concentration of paramagnetic centers.

2. Experimental Section

A. Materials. Sample preparation was as follows: preceramic polymer and ceramic samples of $SiBN_3C$ were synthesized at several pyrolysis temperatures from the single-source precursor TADB (trichlorosilyl-amino-dichloroborane, $Cl_3Si(NH)BCl_2$) with unlabeled methylamine or 99% ^{13}C,^{15}N-labeled methylamine. When TADB and methylamine reacts, methyl-ammoniumchloride immediately precipitates. After all excess amounts of methylamine are evaporated, methyl-ammoniumchloride is removed under vacuum. The complete synthesis scheme of unlabeled and ^{13}C,^{15}N-labeled samples is described elsewhere.[7,10,11] Five different samples were prepared for our studies (see also Table 1). All sample preparations were done under inert atmosphere with the Schlenk technique to avoid contamination by oxygen and water. Sample 1a is a preceramic polymer prepared at a pyrolysis temperature of 673 K. For sample 2a, the polymerized sample was subsequently pyrolyzed at 873 K with a dwell time of 3 h. Sample 2b was prepared under the same conditions as sample 2a except that ^{13}C, ^{15}N-labeled methylamine was used instead of natural abundance methylamine. The samples 3a (natural abundance) and 3b (carbon as a 99% carbon-13 and assuming a fully networked polymer, nitrogen as a 28.6% nitrogen-14 and 71.4% of nitrogen-15) were prepared by pyrolysis of the sample at 1173 K for a dwell time of 3 h at a rate of 5 K/min and subsequent calcination for another 3 h at 1673 K.

B. Methods. Superconducting Quantum Interference Device (SQUID) experiments were performed with MPMS SQUID equipment in the temperature range from 4 to 300 K. All measurements were recorded with an applied magnetic field of 1 T for the samples 1a, 2a, and 3a.

Electron paramagnetic resonance (EPR) experiments were performed on a Bruker EMX cw-X band spectrometer with a microwave frequency of 9.5 GHz from 2 to 293 K with a liquid helium flow cryostat. The experimental parameters were constant for all spectra recorded at various measurement temperatures. The power was kept at 0.16 mW to avoid saturation of signals. The spin concentration and *g*-value were calibrated by use of a standard sample (ultramarine blue diluted by KCl, *g*-value of 2.033). The data processing was performed with the WinEPR software package. All samples were kept under inert atmosphere in a quartz EPR ampule before the measurement.

Solid-state NMR experiments were executed on a Bruker DSX 400 spectrometer operating at 9.4 T with 4 mm triple-resonance (HXY) probe at room temperature. The resonance frequency was 100.60 MHz, and chemical shifts are reported relative to TMS for ^{13}C. All solid-state NMR spectra were acquired by a rotor-synchronous Hahn-echo pulse sequence to remove the probe background signal and eliminate dead time problem. The repetition delay was 30 s for all spectra. The NMR data were processed with matNMR.[12]

3. Results and Discussion

A. Concentration of Paramagnetic Centers. *1. Magnetic Susceptibility Measurements.* Magnetization measurements were performed using a superconducting quantum interference device (SQUID). In Figure 1, the temperature dependence of the magnetic susceptibility (χ) for the unlabeled samples pyrolyzed at various temperatures (673, 873, and 1673 K) is shown. The diamagnetism of the sample is typically evaluated using the Pascal-Langevin formula[13] by considering the combined contribution of several components with the chemical bonding. Since paramagnetic behavior dominates, the total magnetic susceptibility can be quantified by fitting the temperature data to the following equation (eq 1):

$$\chi = \chi_D + \chi^{Pauli} + \chi^{Curie} = \chi_0 + \frac{C}{T-\theta}[\chi - \chi_D - \chi^{Pauli}]^{-1} = \frac{T-\theta}{C} \quad (1)$$

where χ_0 is the temperature independent susceptibility which is composed of χ_D (the diamagnetic susceptibility), χ^{Pauli} (Pauli susceptibility), and χ^{Curie} (Curie−Weiss term, where C is the Curie constant and θ is the Weiss temperature). The results of the fits are summarized in Table 2. The fitting data show that θ values adapt −0.7, −1.9, and −1.2 K for samples pyrolyzed at 673, 873, and 1673 K, respectively. These values correspond to very weak antiferromagnetic interactions, which mean that there is little interaction between the electron spins and that most of them are spatially well separated. Since the χ_D term is already subtracted from the curve of the magnetic susceptibility (χ), the χ^{Pauli} term is the only one which contributes to the temperature independent part of magnetic susceptibility (χ_0). The spin concentration N_S can be obtained by

$$C = \frac{N_S g^2 J(J+1)\mu_B{}^2}{3k_B} \quad (2)$$

where g is the Landé factor ($g = 2$), μ_B denotes the Bohr magneton, and k_B indicates the Boltzmann constant. Several points arise from these data. First, the data suggests a temperature independent susceptibility (χ_0) that increases with the pyrolysis temperature (see Table 2), indicating an increase of electron delocalization. It remains relatively low; for comparison, the Pauli paramagnetic susceptibility of graphite nanoparticles reported in the literature is around $\chi^{Pauli} = +2 \times 10^{-6}$ emu/g.[14]

Second, the concentration of paramagnetic centers is calculated as 3.1×10^{18} spins/g, which corresponds to an average spin−spin distance of 6.2 nm for the sample of the highest spin concentration (sample pyrolyzed at 1673 K) assuming a homogeneous spin distribution over the sample.

(10) Sehlleier, Y. H.; Verhoeven, A.; Jansen, M. *Angew. Chem., Int. Ed.* **2008**, *47*, 3600.
(11) Jansen, M.; Kroschel, M. *Z. Anorg. Allg. Chem.* **2000**, *626*, 1634.
(12) van Beek, J. D. *J. Magn. Reson.* **2007**, *187*, 19.
(13) Lüken, H. *Magnetochemie: Eine Einführung in Theorie und Anwendung*; B. G. Teuner Verlag: Stuttgart, Leipzig, 1999.
(14) Enoki, T.; Andersson, O. E.; Prasad, B. L. V.; Sato, H.; Hishiyama, Y.; Kaburagi, Y. *Phys. Rev. B* **1998**, *58*, 16387.

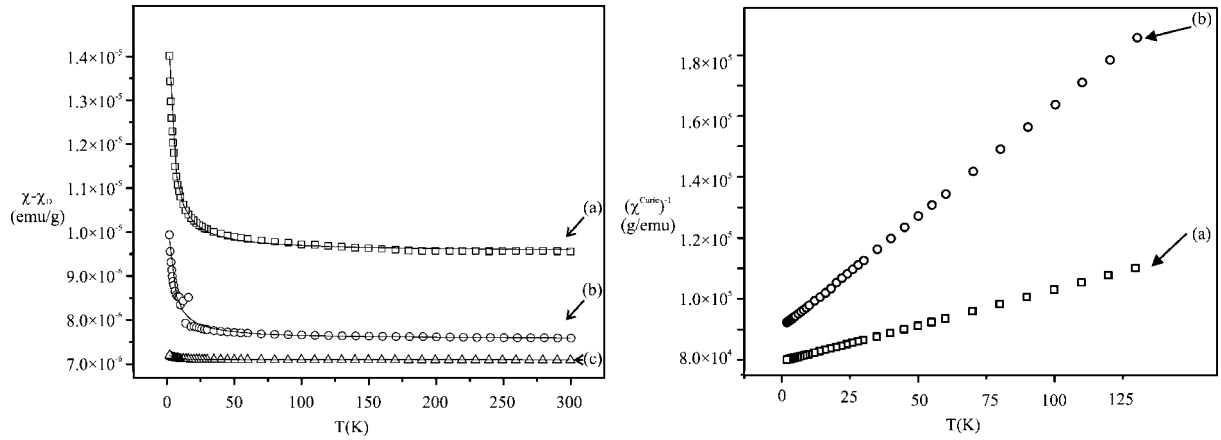

Figure 1. Magnetic susceptibility ($\chi - \chi_D$) versus temperature (left) and the inverse magnetic susceptibility (χ^{Curie})$^{-1}$ versus temperature (right) in a magnetic field $H = 1$ T of unlabeled samples pyrolyzed at (a) 1673, (b) 873, and (c) 673 K, respectively. χ_D: diamagnetic susceptibility, $\chi^{Curie} = \chi - \chi_D - \chi_0$.

Table 2. Summary of Fitting Parameters, Using Equation 1, for the Temperature Dependence of the Magnetic Susceptibility $\chi - \chi_D$ (emu/g)

sample (K)	χ_D (10^{-6} emu/g)	χ_0 (10^{-6} emu/g)	θ (K)	number of spins by SQUID (spins/g)	number of spins by EPR (spins/g)
673	−8.3	+ 0.08	−0.7	6.6×10^{15}	
873	−8.3	+ 0.75	−1.9	4.2×10^{17}	6.9×10^{16}
1673	−8.3	+ 0.96	−1.2	3.1×10^{18}	4.7×10^{18}

Since the distance between paramagnetic centers is rather large, spin exchange interactions are not expected. However, it should be noted that the information by SQUID measurement gives only the overall magnetization in the sample but not the local environment of a particular paramagnetic center.

2. EPR Measurements. The EPR spectra of samples 1a, 2a, and 3a recorded at 10 K are shown in Figure 2. The results clearly show that the concentration of paramagnetic centers is very different in the three samples prepared at various pyrolysis temperatures. Sample 1a is almost "EPR silent" (Figure 2 a), hence, almost no paramagnetic centers have appeared yet for the preceramic polymer at 673 K. This

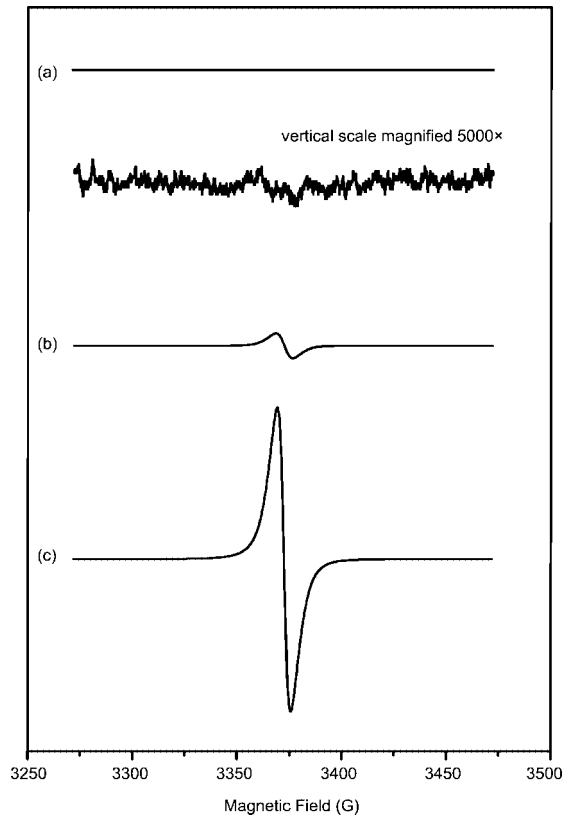

Figure 2. EPR spectra of the unlabeled sample pyrolyzed at (a) 673, (b) 873, and (c) 1673 K, measured at 10 K.

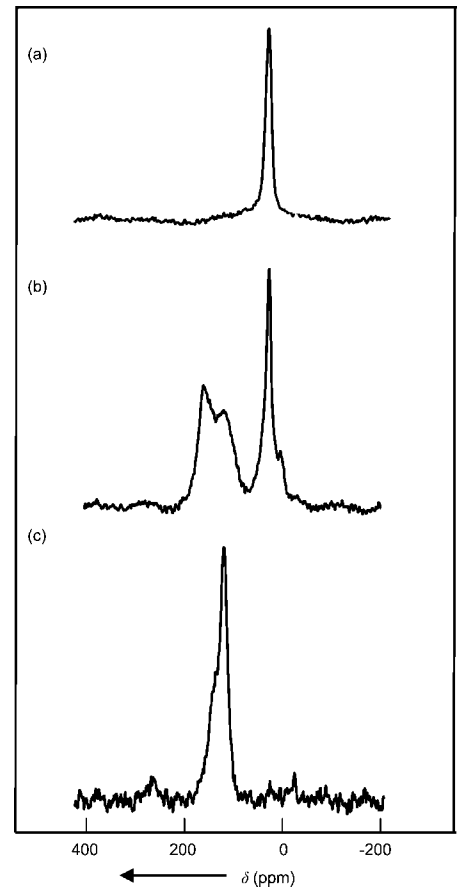

Figure 3. ^{13}C solid-state NMR spectra of the ^{13}C, ^{15}N-labeled samples pyrolyzed at several temperatures, $\omega_r/(2\pi) = 14$ kHz. All spectra are recorded with Hahn-echo pulse sequence. Sample pyrolysis temperatures: (a) 673 K (64 transients), (b) 873 K (80 transients), and (c) 1673 K (1024 transients).

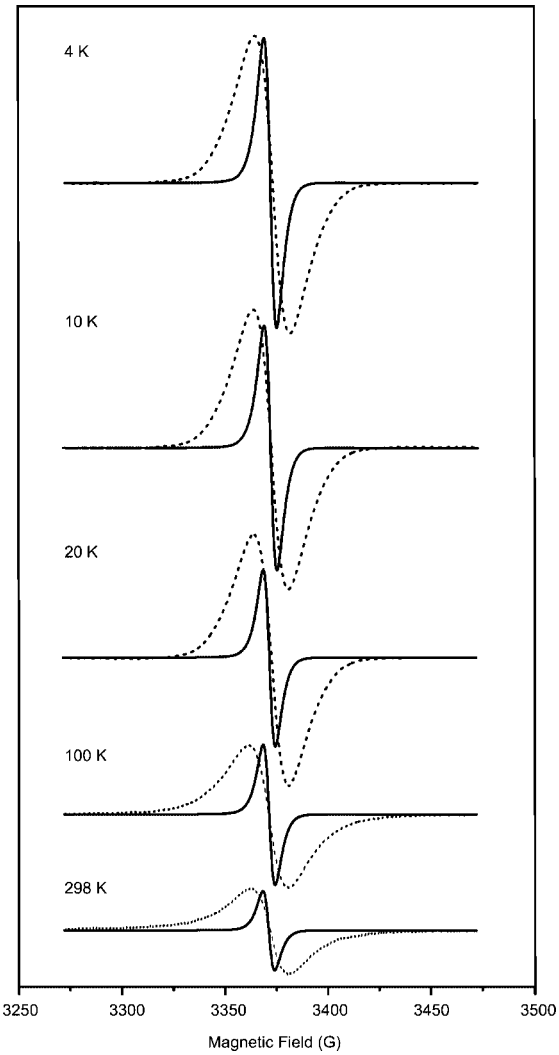

Figure 4. EPR spectra at various measurement temperatures for unlabeled (solid line) and ^{13}C, ^{15}N-labeled (dotted line) samples pyrolyzed at 873 K.

result also indicates that no significant amount of paramagnetic impurities has been introduced during the synthesis. In contrast, EPR spectra of the sample pyrolyzed at 873 K (sample 2a) and 1673 K (sample 3a) (Figure 2 b,c) show strong EPR signals. Only a single resonance was observed, no other signals could be detected over a large magnetic field range. The observed EPR signal can be attributed to carbon-centered paramagnetic centers for the sample pyrolyzed at 873 K (*g*-value of 2.0026) and the sample pyrolyzed at 1673 K (*g*-value of 2.0028). These g-values are typical for carbon centered radicals.[8,9] The spin concentration (measured at 10 K) of the unlabeled sample pyrolyzed at 873 K (sample 2a) was calculated as 6.9×10^{16} spins/g. The spin density increases for the sample pyrolyzed at 1673 K to 4.7×10^{18} spins/g corresponding to an average spin−spin distance of 5.4 nm. This value for the spin concentration agrees with SQUID results and indicates that no large EPR silent paramagnetic fraction is present.

B. Structure Transformation of Carbon Studied by Solid-State NMR. The short and intermediate range ordering of ^{13}C, ^{15}N-labeled SiBNC ceramic has been intensively studied in former work by solid-state NMR.[7,10] Carbon is the only element which shows significant structural changes

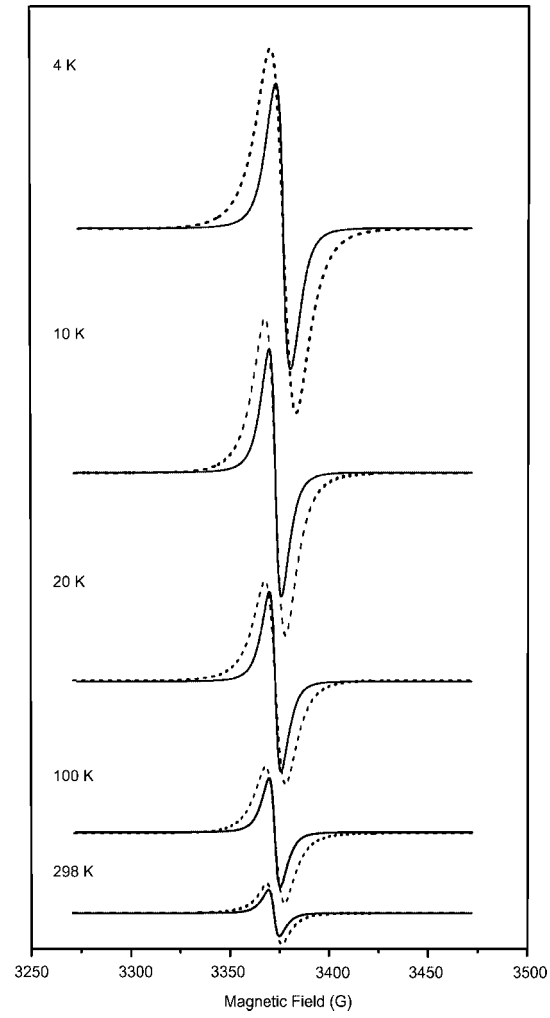

Figure 5. EPR spectra at various measurement temperatures for unlabeled (solid line) and ^{13}C, ^{15}N-labeled (dotted line) samples pyrolyzed at 1673 K.

(boron and silicon exist as BN_3 and SiN_4 in the polymer and they remain in this configuration throughout the pyrolysis). Hence, this variation of the carbon structures may relate to the origin of the paramagnetic character of our sample, and ^{13}C spectra with samples pyrolyzed at different temperatures were recorded (see Figure 3).

The spectra show that the carbon structure changes from fully sp^3-hybridized at 28 ppm via partly sp^2-hybridized to fully sp^2-hybridized from 120 ppm to 160 ppm over the course of the pyrolysis process. In the polymer, carbon is exclusively present as methyl groups, but as the pyrolysis temperature rises they become incorporated into sp^2-hybridized networks. The two components of the peak at around 160 ppm and 120 ppm in Figure 3b seem to correspond to species that are connected to nitrogen and species that have only carbon neighbors, although there are likely to be more unresolved components. On the basis of these and other NMR measurements, we proposed that carbon forms small polycyclic aromatic carbon segments connected with the rest of the material over nitrogen bridges.[7,10]

The transformation of the carbon structure could function both as a source and as a sink for free radicals. Solid-state NMR measurements are complicated by the fact that delocalized segments that contain paramagnetic centers are likely

Table 3. Summary of Fitting Parameters for the Samples Pyrolyzed at 873 and 1673 K Using Mixed Lorentzian/Gaussian Line Shapes Recorded at 4 and 298 K, Respectively[a]

EPR measurement temperature (K)	sample no./pyrolysis temperature (K)	resonance position (G)	line width (G)	fraction Lorentzian component	intensity (%)
4K	2a/873	3373	11.7	0.69	100
	2b/873	3373	17.6	0.39	29.6
		f	31.6	0.00	70.4
	3a/1673	3376	10.9	0.91	100
	3b/1673	3373	14.0	0.57	63.7
		3372	26.7	0.01	36.3
298K	2a/873	3373	10.9	0.75	100
	2b/873	3371	31.9	0.90	100
	3a/1673	3372	9.6	0.96	100
	3b/1673	3373	12.1	1.00	100

[a] Some spectra cannot be fitted satisfactorily by a single peak, therefore an additional component was used.

Table 4. Summary of Fitting Parameters for the Unlabeled and ^{13}C, ^{15}N-Labeled Samples Pyrolyzed at 1673 K Using Mixed Lorentzian/Gaussian Line Shapes Recorded at 2 K

EPR measurement temperature (K)	sample no./pyrolysis temperature (K)	resonance position (G)	line width (G)	fraction Lorentzian component	intensity (%)
2K	3a/1673	3376	4.9	0.94	4.0
		3376	13.6	0.79	96.0
	3b/1673	3374	6.5	0.94	7.5
		3381	19.7	0.52	47.2
		3367	19.9	0.40	45.3

to be invisible in the NMR spectrum. Larger carbon segments are probably more likely to contain a paramagnetic center, reducing the signal-to-noise ratio of the carbon NMR spectrum.

C. Analysis of Line Width and Line Shape of EPR Spectra. In most cases the material only gives a single EPR line, and even taking the second derivative of the absorption spectrum does not reveal any structure in the spectrum. However, it may be possible to detect unresolved interactions between electron spins and nuclear spins by analyzing the line width and line shape of EPR spectra with different labeling schemes, pyrolysis temperatures, and measurement temperatures. This may reveal information on the location of paramagnetic centers. The EPR spectra of unlabeled and ^{13}C, ^{15}N-labeled samples at different pyrolysis temperatures (873 K, 1673 K) are compared in Figures 4 and 5. The normalized EPR spectra were fitted using the derivative of a mixed Lorentzian/Gaussian function $Y'(B)$:

$$Y'(B) = \eta_A L'(B) + (1 - \eta_A) G'(B) \qquad (3)$$

In eq 3, $L'(B)$ is the derivative of a Lorentzian peak, $G'(B)$ is the derivative of a Gaussian peak, and η_A is the Lorentzian character of the mixed peak $Y'(B)$. The full width at half-maximum (fwhm) of $L(B)$ and $G(B)$ (in absorption mode) are kept identical. The Lorentzian line shape occurs when the EPR absorption lines are broadened by the result of the superposition of homogeneous interactions (e.g., dipolar interactions between electrons)[15] or relaxation. The Gaussian line shape arises if the sample includes a superposition of commuting interactions, which would be the case with multiple unresolved, partly anisotropic, hyperfine interactions.[16] Therefore, the deconvolution of Lorentzian/Gaussian line shapes of our EPR spectra can give useful information for the understanding of the line-broadening mechanism in our samples.

The fitting parameters using eq 3 are summarized in Table 3. Some important conclusions can be derived from these results.

The EPR spectra show clear variations in line width (ΔG) depending on the various synthesis conditions. First, generally broader lines are observed for the ^{13}C, ^{15}N-labeled sample compared to the unlabeled sample. This result suggests that the paramagnetic centers are associated with carbon and/or nitrogen. The samples pyrolyzed at high temperature (1673 K) show narrower lines than those pyrolyzed at lower temperature (873 K). It may be due to loss of hydrogen during the pyrolysis process leading to less hyperfine interactions to ^{1}H.

Typical values for isotropic ^{13}C hyperfine couplings are on the order of 20 G, and in the isotope-labeled sample a superposition of hyperfine couplings to several nuclei is expected for most unpaired electrons. The broadening on isotopic enrichment is less than one would expect for such a superposition. Although spin exchange was not expected considering the low spin concentration, this result indicates that spin exchange does play a role and some pairs of electron spins are sufficiently close to interact. The dynamics in the material are not sufficient to generate strong line narrowing at higher measurement temperatures. However, partial averaging is taking place as which manifests itself by the line shape becoming Lorentzian.

The broad peak of the ^{13}C, ^{15}N-labeled sample pyrolyzed at both 873 and 1673 K recorded at low temperature (4 K) has a purely Gaussian line shape which is consistent with line broadening dominated by unresolved hyperfine interactions to carbon and nitrogen. This strong Gaussian contribution is only observed for the ^{13}C, ^{15}N-labeled samples. In the unlabeled samples, because of the absence of unresolved hyperfine couplings, the line shape seems to be dominated by relaxation, leading to a Lorentzian line shape.

D. EPR Spectrum of Labeled Ceramic at 2 K. A uniquely shaped spectrum is observed for sample 3b

(15) Barklie, R. C.; Collins, M. *Phys. Rev. B* **2000**, *61*, 3546.
(16) Barney, L.; Bales, M. P.; Maria Teresa, L. F. *J. Magn. Reson.* **1998**, *132*, 279.

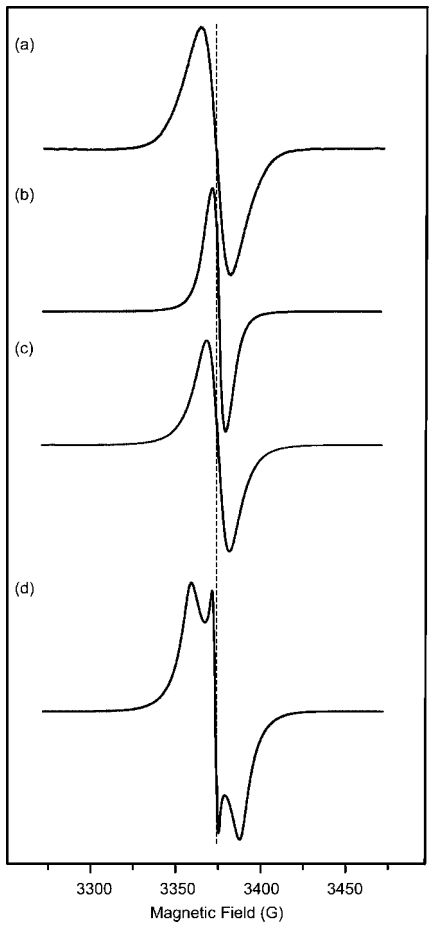

Figure 6. EPR spectra of the unlabeled and ^{13}C, ^{15}N-labeled samples pyrolyzed at 873 and 1673 K. (a) ^{13}C, ^{15}N-labeled sample pyrolyzed at 873 K (2b) recorded at 2 K, (b) unlabeled sample pyrolyzed at 1673 K (3a) recorded at 2 K, (c) ^{13}C, ^{15}N-labeled sample pyrolyzed at 1673 K (3b) recorded at 4 K, and (d) ^{13}C, ^{15}N-labeled sample pyrolyzed at 1673 K (3b) recorded at 2 K.

recorded at 2 K (Figure 6d). All other spectra contain just a single peak, but this particular spectrum seems to contain a clearly distinguishable small sharp peak on top of a broad component. This special form of the EPR spectrum appears at 2 K, and it is not present in the EPR spectrum of the same sample measured at 4 K (Figure 6c). Figure 6 also shows EPR spectra at 2 K of samples 2b and 3a. As was already described, samples 3a and 3b are synthesized under the same conditions except the isotopic labeling scheme of carbon and nitrogen, while 2b is an isotope labeled sample pyrolyzed at a lower temperature. Since EPR spectra of unlabeled and ^{13}C, ^{15}N-labeled samples show a difference, we naturally assume that the origin of the distinct EPR signal of sample 3b is related to the isotopic enrichment of carbon and nitrogen but also by the particular structure of the ceramic that is reached at the final pyrolysis temperature. In Figure 7, the comparison of the experimental and simulated EPR spectra is shown. First, an attempt was made to fit the EPR spectrum with two components, a narrow and a broad one, but this does not result in a good match. Thus, the simulation was repeated with one narrow peak (~6 G) and two broad peaks (~19 G), leading to a more satisfying result (Figure 7b). The fitting parameters are presented in

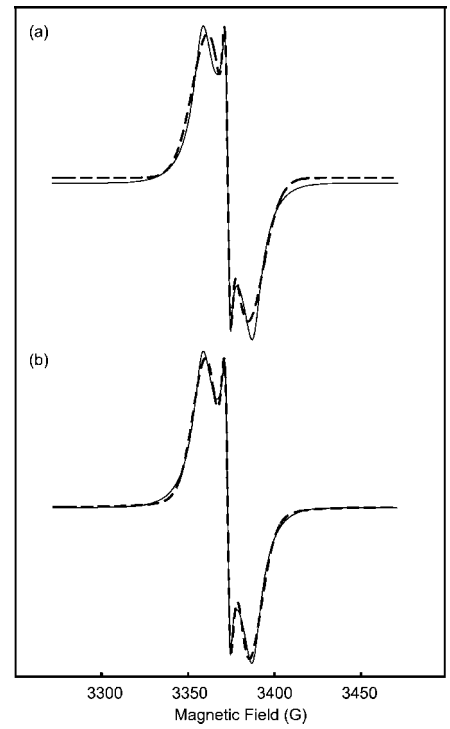

Figure 7. Experimental EPR spectra and sum of simulated spectra of samples pyrolyzed at a temperature of 1673 K. (a) The experimental (solid line) and simulated (dashed line) with one narrow and one broad peak, (b) The experimental (solid line) and simulated (dashed line) with three peaks.

Table 4. The large difference in intensity between the narrow component and the sum of the two broad components make it impossible that these belong to a single multiplet. What would be consistent with the data is the freezing out of states in which the electron is localized on a certain atom. The sharp component would then be the result of the electron spin coupling to a $m_S = 0$ state of a ^{14}N nucleus. Electron spins coupling to the $m_S = 1$ and the $m_S = -1$ states would be broadened by the presence of anisotropic hyperfine interactions. The largest part of these localized unpaired electrons would be positioned near a ^{13}C nucleus, giving rise to a broad doublet. We can only speculate about why this peculiar line shape only appears at this low measurement temperature. The driving force behind the localization process may be the strain exerted on the conjugated segments by the rest of the network. At low measurement temperatures, the surrounding rigid network may force these segments into a shape in which delocalization is no longer possible. This phenomenon probably also occurs in the unlabeled material, but in this case the spectrum does not show resolved resonances because the line width of the electron spins that are not positioned at a ^{14}N nucleus is much narrower due to the lack of hyperfine interactions.

However, it should be noted that it is possible to fit the 2 K spectrum of sample 3a with a broad and a narrow component also (see Table 4). This yields values for the line width for the narrow component and the intensity ratio between the components that is close to that of sample 3b.

Thus, due to broadening by extra hyperfine interactions in the isotope labeled ceramic, effects that could be a

consequence of chemical exchange between localized and delocalized unpaired electrons could be observed.

4. Conclusion

The EPR spectrum of ternary SiBN ceramic showed a very weak signal and originated from some impurities introduced during synthesis,[8] while the signal in the case of quaternary SiBNC ceramic is much stronger and therefore must be associated with the introduction of carbon into the network. The form in which carbon is present in the polymer is very different as compared to its form in fully pyrolyzed ceramic. To reach its final configuration a considerable amount of bond-breaking and bond-forming needs to take place. Obviously, during this process paramagnetic centers are introduced in the system. Berger et al. reported that the EPR intensity of their SiBNC ceramic at a pyrolysis temperature of 1673 K is 14 times lower than at 873 K.[9] In our sample the EPR intensity rises between 873 and 1673 K. This difference can be explained by the use of a different precursor system. In the case of poly(allylmethylsilazane) used by Berger et al.,[9] an even greater atomic rearrangement is required to reach the final structure of the ceramic than in the case of methylpolyborasilazane of our sample. This leads to the formation of more unpaired electrons at intermediate pyrolysis stages. Above a certain temperature the concentration drops again to reach an equilibrium concentration characteristic of SiBNC ceramic of a certain composition.

Comparing the experimental results from unlabeled and ^{13}C, ^{15}N-labeled samples made it possible to draw a conclusion about the location of the unpaired electrons. Carbon is present in the form of small polycyclic aromatic segments. These segments function as sinks for these unpaired electrons, as indicated by the broadening by hyperfine interactions to carbon, and possibly to nitrogen. This could explain the stability of this material at high temperatures.

Acknowledgment. This work is supported by DFG (Deutsche Forschungsgemeinschaft) through the Graduate College of "Modern Methods of Magnetic Resonance in Material Science". We specially thank Prof. Dr. Pavel E. Kazin at the Moscow State University for the SQUID measurements.

CM801889W